ISSN 0030-400X, Optics and Spectroscopy, 2018, Vol. 124, No. 4, pp. 494–500. © Pleiades Publishing, Ltd., 2018.
Original Russian Text © D.A. Volgina, E.A. Stepanidenko, T.K. Kormilina, S.A. Cherevkov, A. Dubavik, M.A. Baranov, A.P. Litvin, A.V. Fedorov, A.V. Baranov, K. Takai, P.S. Samokhvalov, I.R. Nabiev, E.V. Ushakova, 2018, published in Optika i Spektroskopiya, 2018, Vol. 124, No. 4, pp. 477–483.

CONDENSED-MATTER SPECTROSCOPY

# A Study of the Optical Properties of CdZnSe/ZnS-Quantum Dot–Au-Nanoparticle Complexes

**D. A. Volgina[a], E. A. Stepanidenko[a], T. K. Kormilina[a], S. A. Cherevkov[a], A. Dubavik[a], M. A. Baranov[a], A. P. Litvin[a], A. V. Fedorov[a], A. V. Baranov[a], K. Takai[b], P. S. Samokhvalov[c], I. R. Nabiev[c], and E. V. Ushakova[a, *]**

[a] *ITMO University, St. Petersburg, 197101 Russia*

[b] *Hosei University, 3-7-2 Kajino, Koganei, 1848584 Tokyo, Japan*

[c] *Laboratory of Nano-Bioengineering, National Research Nuclear University MEPhI, Moscow, 115409 Russia*

**e-mail: el.ushakova@gmail.com*

Received November 25, 2017

**Abstract**—The interaction of gold nanoparticles (NPs) and semiconductor alloyed CdZnSe/ZnS quantum dots (QDs) in colloidal solutions is studied. It is shown that the photoluminescence intensity of QDs in a mixture decreases compared to that in the initial QD solution, which is caused by resonance nonradiative energy transfer from QDs to Au NPs in spontaneously formed aggregates. To control the formation of pairs of interacting QDs and Au NPs, we proposed have a method for creating QD–Au NP complexes bound by special molecules—ligands. It is shown that the morphology and optical properties of the samples obtained depend on the method of their preparation, in particular, on the chemical environment of QDs. It is found that the complexes form in the case of addition of hydrophilic Au NPs to hydrophobic QDs and that this almost does not change the optical properties of the latter compared to those of quasi-isolated QDs in colloidal solution.

**DOI:** 10.1134/S0030400X18040185

## INTRODUCTION

One of the directions of development of modern materials science is the development of nanostructured hybrid materials with outstanding physical and chemical properties. Due to the rapid development of the methods of synthesis of nanostructured materials in the last decade, it became possible to create nanoparticles (NPs) of various shapes, sizes, and chemical compositions with unique optical responses [1–8]. The combination of these excellent properties opens up the possibility of creating materials with a prescribed set of parameters needed for their application. In particular, this has allowed one to create multicomponent hybrid materials based on systems of interacting nanoobjects, such as quantum dot (QD) ensembles [9–11], complexes of NPs with graphene [12, 13], and complexes of magnetic NPs with QDs [14, 15], dielectric NPs [16, 17], metal NPs and QDs [18–21], etc.

Hybrid complexes based on metal NPs and semiconductor QDs attract particular interest because the unique optical properties of QDs, such as high photoluminescence (PL) quantum yields and high extinction coefficients in a wide spectral range, are enhanced due to local fields near metal NPs. These materials are promising for application in photonics devices, namely, in solar and photocatalytic cells [22]. Another field of possible applications of these materials is the use of them as biological sensors [23, 24], including selective probing of amino acids [19]. In addition, these QD–NP hybrid complexes can be used to improve visualization of biological tissues by optical microscopy [25, 26]. Thus, the development of formation protocols of QD–NP hybrid complexes in colloidal solutions with controlled morphological parameters is an important problem.

In the present work, we study the interaction of CdZnSe/ZnS semiconductor alloyed QDs with Au NPs in colloidal solutions and the change of their optical properties depending on the morphology of the formed complexes.

## EXPERIMENTAL METHODS

The spectral analysis of the samples of QDs and gold NPs in solution, as well as of the complexes formed on substrates, was performed using a UV-3600 spectrophotometer (Shimadzu), a Cary Eclipse spectrofluorimeter (Varian), and an LSM-710 confocal microscope (Zeiss). The morphology of the formed complexes was studied with a Merlin electron microscope (Zeiss). The luminescent images and transmission microphotographs of the samples were obtained using an LSM-710 confocal microscope (Zeiss). The

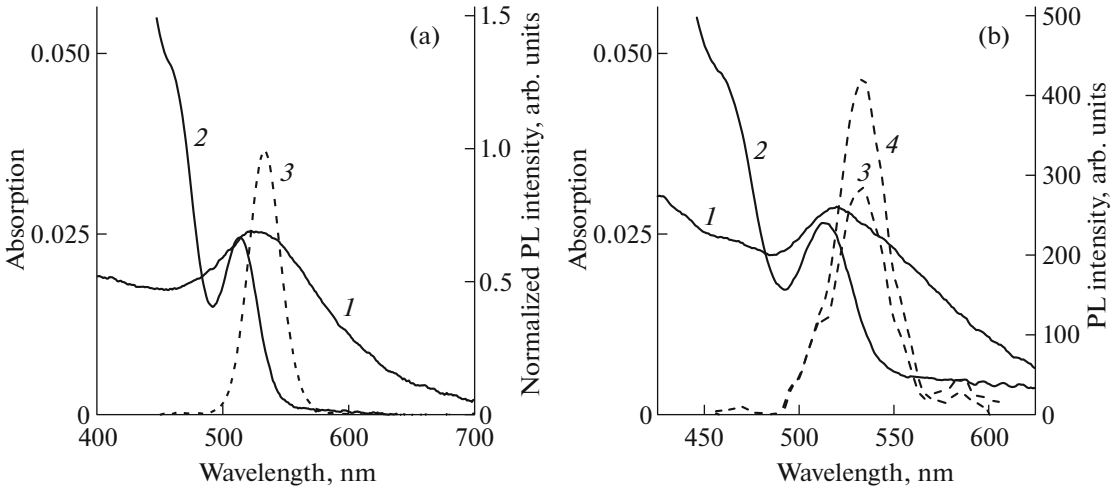


**Fig. 1.** (a) Absorption (solid lines) and PL (dashed line) spectra of the initial colloidal solutions of (*1*) Au NPs and (*2*, *3*) QDs; (b) absorption (solid lines) and PL (dashed line) spectra of the (*1*, *3*) sNP + QD and (*2*, *4*) sQD + NP solutions with the maximum addition of the second component.

PL-decay kinetics was studied using a MicroTime100 confocal microscope (PicoQuant) by the time-correlated single-photon-counting method.

## MATERIALS

In this work, we used colloidal alloyed CdZnSe/ZnS QDs. They were formed by organometallic synthesis in organic solution by the method described in [27]. As a result, we synthesized QDs with a diameter of 7.0 ± 1.0 nm stabilized by organic ligand molecules—trioctylphosphine oxide (TOPO) and oleic acid (OA), with chains 1.3 and 1.8 nm long, respectively. Colloidal gold NPs were synthesized by the method described in [28]. The synthesized NPs were 6.0 ± 0.8 nm in size and were stabilized by polyethylene glycol (PEG) with a chain length of 3.5 nm. The absorption and PL spectra of the colloidal solutions of nanocrystals in organic solvents are presented in Fig. 1a.

To study the interaction of quasi-isolated colloidal nanocrystals with initial ligand molecules in organic solvent, we prepared two series of samples. The first series, hereinafter denoted as sQD + NP, was prepared by adding a solution of Au NPs by portions of 10 μL to a QD solution, the maximum added volume being 100 μL. The samples of the second series, denoted as sNP + QD, were, vice versa, prepared by adding a QD solution to a solution of Au NPs. The absorption and PL spectra were recorded after each addition. Figure 1b presents the recorded absorption and PL spectra of the two solutions obtained with the maximum addition. It is seen that the PL band is almost the same in both cases except for its intensity. The band intensity linearly increases for the sNP + QD series and linearly decreases for the sQD + NP series.

To understand whether QDs and Au NPs interact in the mixture of solutions, we compared the experimental values of integral PL intensity $S(PL)_{exp}$ with PL intensity $S(PL)_{calc}$ calculated as a function of the contributions of QDs to optical density $D_{QD}$ of the mixture of solutions in the exciton peak (514 nm); i.e., $S(PL)_{calc} = D_{QD}S(PL)^*_{exp}/D_{QD\,sol}$, where $S(PL)^*_{exp}$ and $D_{QD\,sol}$ are the integral PL intensity and the optical density of the initial QD solution, respectively. The contribution of QDs to the optical density of the mixture in the case of addition of their solution into the solution of Au NPs was calculated as $D_{QD} = D_{QD\,sol}V_{QD\,sol}/V_{mix}$, where $V_{QD\,sol}$ and $V_{mix}$ are the volumes of the initial QD solution and of the mixture of solutions, respectively. In the case of addition of QDs into the solution of Au NPs, we have $D_{QD} = D_{QD} - D_{Au}V_{Au}/V_{mix}$, where $D_{Au}$ and $V_{Au}$ are the optical density at a wavelength of 514 nm and the volume of the solution of Au NPs, respectively. The calculated dependences are presented in Fig. 2 in comparison with the experimental data.

The experimental values in both cases are smaller than theoretical, which means that the QD PL is quenched in the presence of gold nanoparticles. We estimated the ratio of the theoretical and experimental data, i.e., the relative quenching coefficient. This value increases with decreasing concentration of QDs in the mixture. This is related mainly to the unwanted and uncontrolled resonance energy transfer from QDs to Au NPs in spontaneously formed aggregates in the mixture of solutions. Against this background, we posed the problem of creating QD–NP complexes bound by organic ligand molecules with a controlled distance between nanocrystals in colloidal solution.

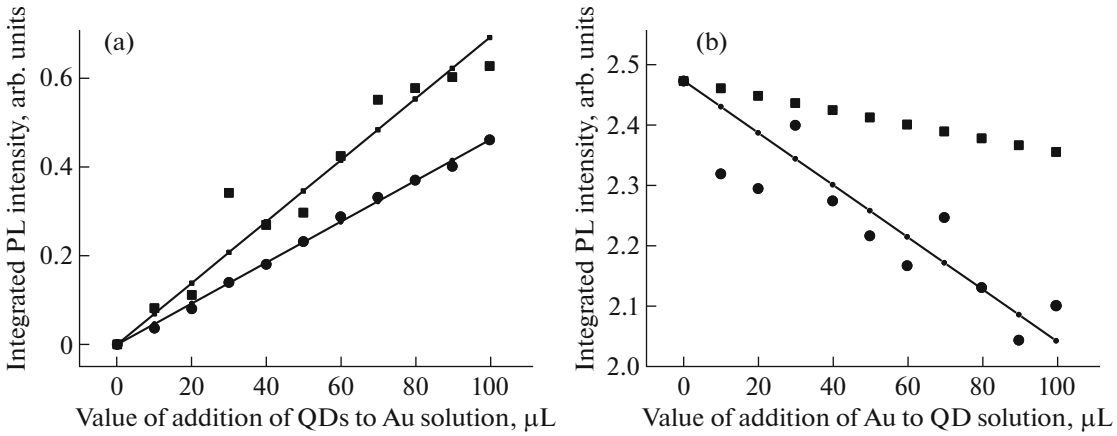


**Fig. 2.** Calculated (squares) and experimental (circles) dependences of the change in the integral QD PL intensity with addition of $N$ μL of the second component for (a) sNP + QD and (b) sQD + NP.

To form colloidal complexes of Au NPs and QDs, it is necessary to use organic molecules with two active groups, namely, the thiol (–SH) and carboxyl (–COOH) groups, which covalently bind to Au and Zn atoms on the surfaces of NPs and QDs, respectively. For this purpose, we chose 4-mercaptobenzoic acid (4MBA) and 6-mercaptohexanoic acid (6MHA) molecules. First, Au NPs were solubilized by the chosen molecules by a method similar to that described in [29]. After solubilization, NPs were dispersed in an aqueous solution with addition of NaOH. For better binding of the chosen ligands with QDs, their surface was preliminarily cleared from the initial ligand molecules—TOPO and OA.

In the first series of the samples, 50 μL of the aqueous solution of NPs was added to 450 of the QD solution in tetrachloromethane (TCM). In the second series, 50 of the QD solution in TCM was added to 450 of the aqueous solution of NPs. For clarity, the sample numbers, as well and the types of solvents and molecules on the surfaces of QDs and Au NPs, are listed in Table 1.

Scanning electrone microscopy (SEM) images of the samples formed by deposition of small amounts of the studied solutions on electron-microscopy grids are shown in Fig. 3. In addition, Fig. 3a shows the microimage of a sample prepared by deposition of the reference solution on a glass substrate.

It is seen that the deposition of the reference solution on a glass substrate results in the formation of disordered structures, in which nanocrystals form large aggregates. The solutions of samples 1 and 2 deposited on the grids form chains consisting of elements of about 10 nm in size (Figs. 3b, 3c). This indicates that Au NPs and QDs bind in the colloidal solution and are deposited in the bound state. In the case of samples 3 and 4, one observes the formation of large filament-like structures consisting of organic molecules, a typical SEM image of which is given in Fig. 3d. Nanocrystals in these samples are chaotically distributed over the area of these filament-like structures (Figs. 3e, 3f). Thus, binding of Au NPs and QDs into complexes in these samples did not occur.

## RESULTS AND DISCUSSION

We obtained microimages of the samples formed by deposition of the obtained solutions on a glass substrate. Figure 4 presents typical luminescence images.

Analysis of the optical microphotographs revealed the formation of small spheres with dimensions of about 10–30 μm in the case of solution of the first series. Quantum dots in sample 1 exist mainly in separate spheres on the substrate. Sample 2 also exhibits a structure with spherical objects, which more resemble micelles. In this case, QDs are distributed over the boundaries of micelles. Compared to the initial solutions, the PL bands of the first and the second samples are shifted to shorter wavelengths by 4 and 8 nm, respectively. The microimages of the samples obtained by deposition of solutions of the second series on a

**Table 1.** Sample numbers and chemical compositions

| Sample | Reference sample | 1 | 2 | 3 | 4 |
|---|---|---|---|---|---|
| Solvent | Toluene | TCM | TCM | $H_2O$ | $H_2O$ |
| QD ligand type | TOPO + OA | – | – | – | – |
| Au NP ligand | PEG | 4MBA | 6MHA | 4MBA | 6MHA |

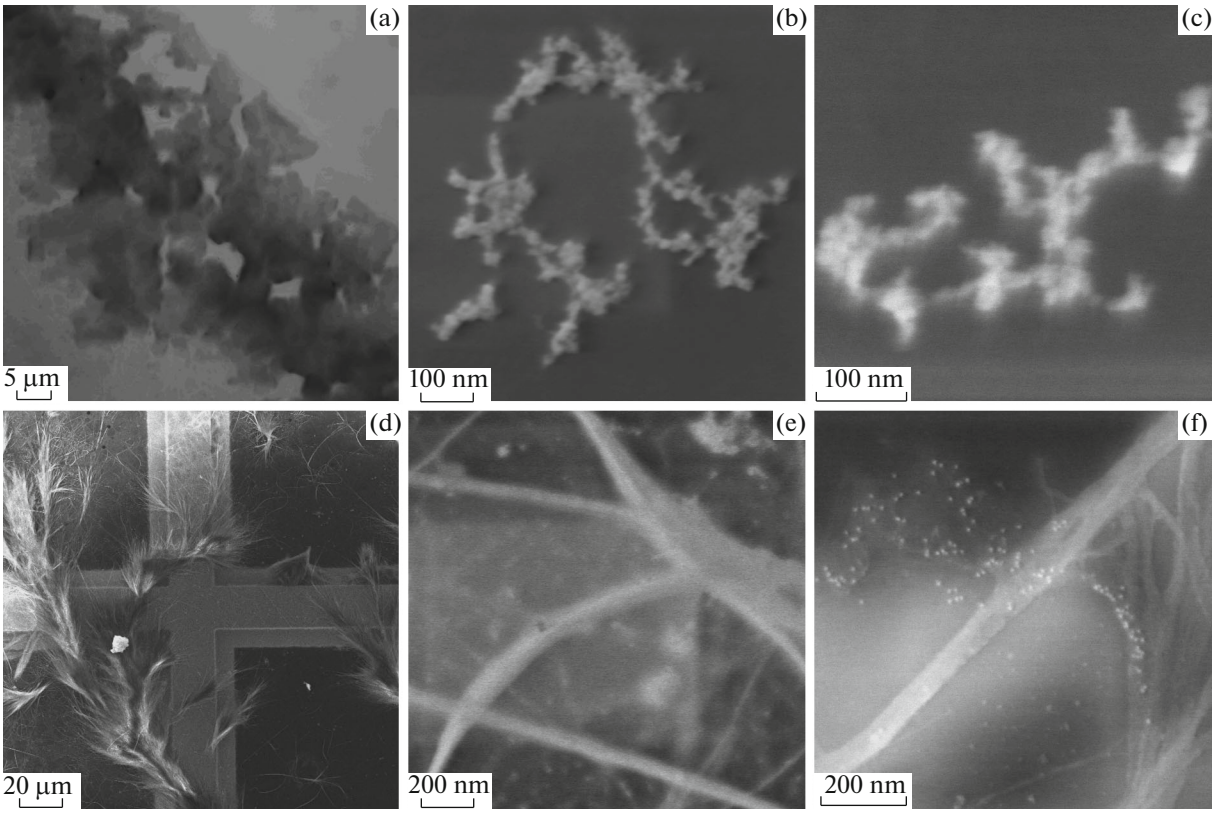


**Fig. 3.** (a) Microimage of reference sample on glass in transmitted light; (b–f) SEM images of samples 1 (b), 2 (c), 3 (d, e), and 4 (f).

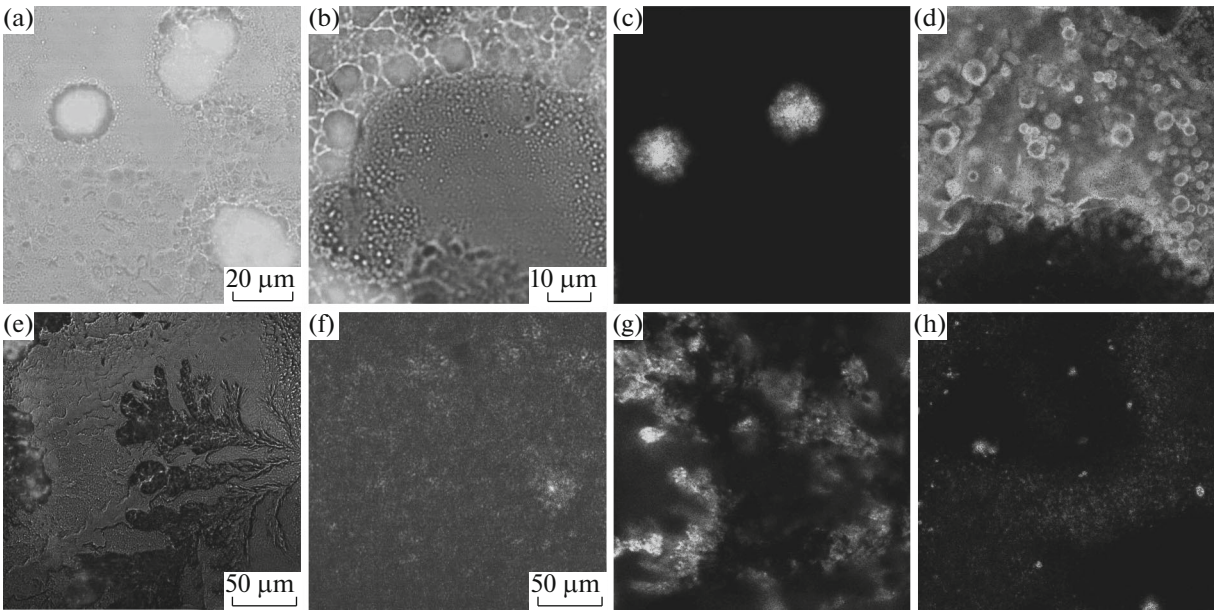


Fig. 4. (a, b, e, f) Superimposition of photoluminescence images on images in transmitted light and (c, d, g, h) 80 × 80 mm fluorescence lifetime images (FLIM) of samples: 1 (a, c), 2 (b, d), 3 (e, g), and 4 (f, h).

**Table 2.** Spectral characteristics of samples in comparison with the initial colloidal solution of QDs

| Sample | Reference sample | 1 | 2 | 3 | 4 | Initial QD solution |
|---|---|---|---|---|---|---|
| morphology | aggregates | bound complexes | | disordered ensembles | | quasi-isolated |
| PL peak, nm | 533 | 530 | 526 | 528 | 529 | 534 |
| PL intensity, arb. units | 10 | 450 | 350 | 100 | 10 | – |
| QD PL lifetime, ns | 13.1 ± 1.5 | 25.5 ± 1.5 | 27.7 ± 0.8 | 26.3 ± 1.0 | 16.0 ± 5.5 | 36.0 ± 2.0 |

substrate show the formation of filament structures (Figs. 4e, 4f), which agrees with the SEM images of the samples deposited on electron-microscopy grids. At the same time, QDs are not incorporated into the structures formed by organic molecules. The PL intensities of samples 3 and 4 decrease with a slight blue shift of the PL band. The positions of the PL bands of the samples are presented in Table 2.

To determine how the presence of an Au NP near a QD, the method of complex formation, and the chemical surrounding of QDs affect their optical properties, we studied the PL decay parameters. We obtained the maps of the PL lifetime time and intensity of the samples. The PL lifetime curve represented the sum of luminescence responses recorded at each point of the region considered. Analysis of the PL decay of the samples showed that the PL decay curves can be described by an exponential dependence of the form $I(t) = \sum_i A_i e^{-t/\tau}$. The average PL lifetime was calculated by the formula $\langle\tau\rangle = \frac{\Sigma A_i \tau_i^2}{\Sigma A_i \tau_i}$. Figure 5 shows the typical PL decay curves of the samples.

First, we studied the optical responses of the reference sample. The PL lifetime is 14.8 ± 1.2 ns in the sNP + QD sample and 11.9 ± 0.9 ns in the sQD + NP sample. To understand how QDs are arranged in aggregates with Au NPs, we plotted the PL decay curves of QDs at different wavelengths within the range of 520–560 nm using interference filters. These curves are shown in Fig. 5a. It was found that the average lifetime was 8.4 ns for a wavelength of 520 nm and 16.8 ns for 560 nm. These dependences indicate that the decrease in the PL lifetime is caused not by interaction with Au NPs but, most probably, by the formation of QD aggregates. In this case, nonradiative energy transfer may occur from smaller QDs to larger ones inside a quasi-monodisperse ensemble of QDs in aggregates.

Figure 5b shows the typical PL-decay curves for samples 1 and 3 in comparison with the initial colloidal solutions of QDs and with the reference sample. It is seen that the average PL lifetimes for QDs in the samples of both series are slightly shorter than those for the initial solution but larger than the decay times for the reference sample. The average PL lifetimes determined by approximation of the PL intensity for all the samples are given in Table 2. The averaging was performed over several regions in each sample.

For the samples of the first series, we observed a slight decrease in the QD PL lifetimes, the average values of which were 25.5 ± 1.5 and 27.7 ± 0.8 ns for samples 1 and 2, respectively. As is seen from Figs. 4c and 4d, the structures formed by the complexes of QDs and Au NPs have approximately identical PL parameters, both intensity and lifetimes. This testifies to a

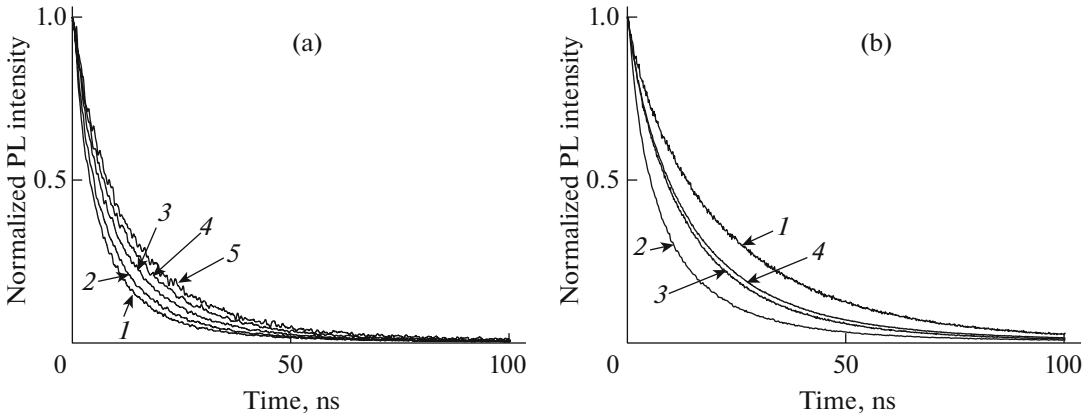


**Fig. 5.** Normalized PL decay curves (a) for an sQD + NP sample at wavelengths of (*1*) 520, (*2*) 530, (*3*) 540, (*4*) 550, and (*5*) 560 nm and (b) for (*1*) the initial QD solution, (*2*) sQD + NP, (*3*) sample 1, and (*4*) sample 3.

uniform distribution of QDs and Au NPs in the structures, which also indirectly confirms the formation of bound complexes in these samples.

In contrast to the first series, the spatial distribution of QD PL parameters for the second series depended on the sample morphology. In Figs. 4g and 4h, one can see separate regions with shorter PL lifetimes and higher relative intensities. However, these brightly luminescent regions made a small contribution to the total signal of PL decay summarized over the entire recorded region. The average PL lifetime for sample 3 was 26.3 ± 1.0 ns. The PL intensity of sample 4 was observed to strongly decrease, which was accompanied by a decrease in the average lifetime to 16.0 ± 5.5 ns. We suggest that this change in the optical properties of QDs in the second series of samples is related to the method of formation of complexes, at which binding of QDs and Au NPs almost does not occur. Therefore, the carboxyl groups of the chosen ligand molecules do not bind to the QD surface instead of the initial TOPO and OA molecules, which leads to the formation of additional channels of nonradiative photoexcitation energy relaxation.

## CONCLUSIONS

We have studied the interaction of gold nanoparticles and semiconductor alloyed QDs in colloidal solutions. It is shown that the QD PL intensity in the mixture decreases compared to the initial QD solution. This is due to the nonradiative resonance-energy transfer from QDs to closely spaced NPs in spontaneously formed aggregates in the mixture. To control the formation of QD–NP pairs, we proposed a method for creating QD–Au NP complexes bound by special ligand molecules in colloidal solution. It is shown that the morphology and the optical properties of the formed samples depend on the method of their preparation, in particular, on the chemical environment of QDs. It is shown that the complexes are formed in the case of addition of hydrophilic gold nanoparticles to hydrophobic QDs and that the optical properties remain almost unchanged compared to quasi-isolated QDs in colloidal solution. To achieve enhancement of the optical signals of QDs in such complexes, it is necessary to perform further investigations to optimize the methods of formation of systems with controlled morphological parameters of QD–NP complexes.

The results obtained in this work will improve the understanding of interaction of components in hybrid nanostructured materials for their successful application in devices of nanooptics and photonics.

## ACKNOWLEDGMENTS

This work was supported by the Ministry of Education and Science of the Russian Federation, projects MK-1757.2017.2, 14.584.21.0032, and 14.B25.31.0002.

## REFERENCES

1. C. R. Kagan, E. Lifshitz, E. H. Sargent, and D. V. Talapin, Science **353** (6302), aac5523 (2016).
2. D. V. Talapin and E. V. Shevchenko, Chem. Rev. **116**, 10343 (2016).
3. S. Neretina, R. A. Hughes, K. D. Gilroy, and M. Hajfathalian, Acc. Chem. Res. **49**, 2243 (2016).
4. J. Owen and L. Brus, J. Am. Chem. Soc. **139**, 10939 (2017).
5. K. Susumu, L. D. Field, E. Oh, M. Hunt, J. B. Delehanty, V. Palomo, P. E. Dawson, A. L. Huston, and I. L. Medintz, Chem. Mater. **29**, 7330 (2017).
6. Z. Hedayatnasab, F. Abnisa, and W. M. A. W. Daud, Mater. Des. **123**, 174 (2017).
7. U. Aslam and S. Linic, Chem. Mater. **28**, 8289 (2016).
8. Y. Kim, B. Yeom, O. Arteaga, S. J. Yoo, S. G. Lee, J. G. Kim, and N. A. Kotov, Nat. Mater. **15**, 461 (2016).
9. A. P. Litvin, A. A. Babaev, P. S. Parfenov, E. V. Ushakova, M. A. Baranov, O. V. Andreeva, K. Berwick, A. V. Fedorov, and A. V. Baranov, J. Phys. Chem. C **121**, 8645 (2017).
10. E. V. Ushakova, S. A. Cherevkov, A. P. Litvin, P. S. Parfenov, D.-O. A. Volgina, I. A. Kasatkin, A. V. Fedorov, and A. V. Baranov, J. Phys. Chem. C **120**, 25061 (2016).
11. E. V. Ushakova, S. A. Cherevkov, A. P. Litvin, P. S. Parfenov, V. V. Zakharov, A. Dubavik, A. V. Fedorov, and A. V. Baranov, Opt. Express, No. 24, A58 (2016).
12. I. A. Reznik, Y. A. Gromova, A. S. Zlatov, M. A. Baranov, A. O. Orlova, S. A. Moshkalev, V. G. Maslov, A. V. Baranov, and A. V. Fedorov, Opt. Spectrosc. **122**, 114 (2017).
13. K. J. Huang, D. J. Niu, X. Liu, Z. W. Wu, Y. Fan, Y. F. Chang, and Y. Y. Wu, Electrochim. Acta **56**, 2947 (2011).
14. A. K. Visheratina, F. Purcell-Milton, R. Serrano-Garcia, V. A. Kuznetsova, A. O. Orlova, A. V. Fedorov, A. V. Baranov, and Y. K. Gun'ko, J. Mater. Chem. C **5**, 1692 (2017).
15. L. Lou, K. Yu, Z. Zhang, B. Li, J. Zhu, Y. Wang, R. Huang, and Z. Zhu, Nanoscale **3**, 2315 (2011).
16. E. Tiguntseva, A. Chebykin, A. Ishteev, R. Haroldson, B. Balachandran, E. Ushakova, F. Komissarenko, H. Wang, V. Milichko, A. Tsypkin, D. Zuev, W. Hu, S. Makarov, and A. Zakhidov, Nanoscale **9**, 12486 (2017).
17. P. A. Dmitriev, D. G. Baranov, V. A. Milichko, S. V. Makarov, I. S. Mukhin, A. K. Samusev, A. E. Krasnok, P. A. Belov, and Y. S. Kivshar, Nanoscale **8**, 9721 (2016).
18. A. Ridolfo, O. di Stefano, N. Fina, R. Saija, and S. Savasta, Phys. Rev. Lett. **105**, 263601 (2010).
19. B. Paramanik, S. Kundu, G. De, and A. Patra, J. Mater. Chem. C **4**, 486 (2016).
20. J. D. Cox and M. R. Singh, Adv. Opt. Mater **1**, 460 (2013).
21. C. Strelow, T. S. Theuerholz, C. Schmidtke, M. Richter, J. P. Merkl, H. Kloust, Z. Ye, H. Weller, T. F. Heinz, A. Knorr, and H. Lange, Nano Lett. **16**, 4811 (2016).

22. Y. S. Chen, H. Choi, and P. V. Kamat, J. Am. Chem. Soc. **135**, 8822 (2013).
23. J. Liu, M. Cui, H. Zhou, and S. Zhang, Sci. Rep. **6**, 30577 (2016).
24. T. Pons, I. L. Medintz, K. E. Sapsford, S. Higashiya, A. F. Grimes, D. S. English, and H. Mattoussi, Nano Lett. **7**, 3157 (2007).
25. U. Resch-Genger, M. Grabolle, S. Cavaliere-Jaricot, R. Nitschke, and T. Nann, Nat. Methods **5**, 763 (2008).
26. E. Petryayeva, W. R. Algar, and I. L. Medintz, Appl. Spectrosc. **67**, 215 (2013).
27. W. K. Bae, J. Kwak, J. Lim, D. Lee, M. K. Nam, K. Char, C. Lee, and S. Lee, Nano Lett. **10**, 2368 (2010).
28. A. Dubavik, V. Lesnyak, N. Gaponik, and A. Eychmüller, Langmuir **27**, 10224 (2011).
29. E. V. Ushakova, T. K. Kormilina, M. A. Burkova, S. A. Cherevkov, V. V. Zakharov, V. K. Turkov, A. V. Fedorov, and A. V. Baranov, Opt. Spectrosc. **122**, 25 (2017).

*Translated by M. Basieva*